

Coordination Chemistry, Structure, and Reactivity of Thiouracil Derivatives of Tungsten(0) Hexacarbonyl: A Theoretical and Experimental Investigation into the Chelation/Dechelation of Thiouracil via CO Loss and Addition

Donald J. Darensbourg,* Brian J. Frost, Agnes Derecskei-Kovacs, and Joseph H. Reibenspies

Department of Chemistry, Texas A&M University, P.O. Box 30012, College Station, Texas 77842-3012

Received June 30, 1999

The synthesis of 2-thiouracil and 6-methyl-2-uracil derivatives of tungsten carbonyl from the reaction of photogenerated $W(CO)_5(\text{solvent})$ (solvent = MeOH or THF) and the corresponding $[Et_4N][\text{thiouracilate}]$ is described. The crystal structure of the $[Et_4N][W(CO)_5(2\text{-thiouracilate})]$, **1**, derivative is reported where the thiouracilate is found to be bound to the tungsten center via the exocyclic sulfur atom. In the solid-state structure of **1** two anions are associated by means of two hydrogen bonds between the metal bound nucleobases. These pentacarbonyl complexes stereoselectively lose cis carbonyl ligands, as is apparent from ^{13}C -labeling studies, to provide the endocyclic nitrogen N(1)-chelated tungsten tetracarbonyl derivatives, e.g., $[Et_4N][W(CO)_4(2\text{-thiouracilate})]$, **3**. The kinetics of the loss of CO from the pentacarbonyl anions to afford the metal tetracarbonyls, and the reverse of that process, were monitored by means of in situ infrared spectroscopy in the $\nu(\text{CO})$ region as a function of temperature. These studies reveal that the tetracarbonyl anions in CO-saturated acetonitrile ($[\text{CO}] \approx 6 \times 10^{-3} \text{ M}$) are unstable with respect to the formation of the pentacarbonyl derivatives, i.e., the equilibrium $\mathbf{1} \rightleftharpoons \mathbf{3} + \text{CO}$ lies to the left under an atmosphere of carbon monoxide. From the activation parameters determined for the dissociative CO loss process ($\Delta H^\ddagger = 82.0 \pm 3.6 \text{ kJ mol}^{-1}$ and $\Delta S^\ddagger = -44.9 \pm 9.6 \text{ J mol}^{-1} \text{ K}^{-1}$ for complex **1**) it is apparent that the sulfur-bound thiouracilate ligand is serving as a π -donor during CO dissociation, i.e., behaving as a cis-labilizing ligand. Ab initio geometry optimizations carried out for the process $\mathbf{1} \rightleftharpoons \mathbf{3} + \text{CO}$ at the Hartree–Fock and DFT levels support these experimental observations. For example, complex **1** is shown to be more stable than **3** + CO and chelation via the endocyclic N(1) donor is favored over N(3) binding. Finally, the “16-electron” intermediate resulting from CO dissociation in **1** was found to possess a significantly shortened W–S interaction, presumably due to the π -donating ability of the thiouracilate ligand.

Introduction

The coordination chemistry of nucleobases to metal centers has been an active area of research for several decades.^{1–3} Most of these studies have dealt with biologically relevant metals in positive oxidation states, such as magnesium, platinum, and cadmium. Generally these efforts have been directed toward the examination of the coordination modes of neutral nucleobases to metals. Nevertheless, there have been several investigations carried out on metal complexes involving the binding of monoanions of the nucleobases. Importantly, this area of research has been pivotal in the gleaning of information about how metal-based drugs such as cisplatin and metallocene dihalides operate.^{4,5} These studies have led to the synthesis of metal complexes which exhibit biological activity. For example, Tiekink and co-workers have shown that thiouracil-containing complexes are effective antitumor and arthritic compounds in

vivo.⁶ A comprehensive understanding of the coordination chemistry of these complexes is necessary for the rational design of other useful uracil-containing metal derivatives.

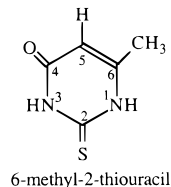
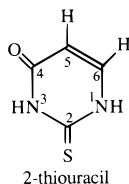
For the last several years we have been investigating the π -donor abilities of various ligands as measured via their propensity for labilizing cis CO ligands in octahedral metal carbonyl derivatives.^{7–14} Included in these studies are complexes containing pseudo amido donor ligands such as $W(CO)_5(\text{uracilate})^-$, where the nucleobases are bound to the metal centers via one of the ring nitrogens.^{7,15} The isolation and infrared spectral properties of several neutral and anionic metal

- (1) Goodgame, M.; Jakubovic, D. A. *Coord. Chem. Rev.* **1987**, *79*, 97.
- (2) Mutikainen, I. *Ann. Acad. Sci. Fenn., Ser. A2* **1988**, *No. 217*, and references therein.
- (3) (a) Lusty, J. R., Ed. *CRC Handbook of Nucleobase Complexes: Transition Metal Complexes of Naturally Occurring Nucleobases and Their Derivatives*; CRC Press: Boca Raton, FL, 1990; Vol. 1, pp 9–99. (b) Bloemink, M. J.; Reedijk, J. In *Interaction of Metal Ions with Nucleotides, Nucleic Acids and Their Derivatives*; Sigel, A., Sigel, H., Eds.; Marcel Dekker: New York, 1996; pp 641–685.
- (4) Murray, J. H.; Harding, M. M. *J. Med. Chem.* **1994**, *37*, 1936–1941.
- (5) (a) Yuriev, E.; Orbell, J. D. *Inorg. Chem.*, **1998**, *37*, 6269–6275. (b) Zangrando, E.; Pinchierrri, F.; Randaccio, L.; Lippert, B. *Coord. Chem. Rev.* **1998**, *156*, 275–332 and references within.

- (6) (a) Cookson, P. D.; Tiekink, E. R. T.; Whitehouse, M. W. *Aust. J. Chem.* **1994**, *47*, 577. (b) Tiekink, E. R. T.; Cookson, P. D.; Linahan, B. M.; Webster, L. K. *Met. Based Drugs* **1994**, 299.
- (7) Darensbourg, D. J.; Draper, J. D.; Larkins, D. L.; Frost, B. J.; Reibenspies, J. H. *Inorg. Chem.* **1998**, *37*, 2538.
- (8) Darensbourg, D. J.; Sanchez, K. M.; Reibenspies, J. H. *Inorg. Chem.* **1988**, *27*, 3636.
- (9) Darensbourg, D. J.; Atnip, E. V.; Klausmeyer, K. K.; Reibenspies, J. H. *Inorg. Chem.* **1994**, *33*, 5230.
- (10) Darensbourg, D. J.; Draper, J. D.; Reibenspies, J. H. *Inorg. Chem.* **1997**, *36*, 3648.
- (11) Darensbourg, D. J.; Klausmeyer, K. K.; Reibenspies, J. H. *Inorg. Chem.* **1995**, *34*, 4676.
- (12) Darensbourg, D. J.; Klausmeyer, K. K.; Reibenspies, J. H. *Inorg. Chem.* **1996**, *35*, 1529.
- (13) Darensbourg, D. J.; Klausmeyer, K. K.; Reibenspies, J. H. *Inorg. Chem.* **1996**, *35*, 1535.
- (14) Darensbourg, D. J.; Klausmeyer, K. K.; Draper, J. D.; Chojnacki, J. A.; Reibenspies, J. H. *Inorg. Chim. Acta* **1998**, *270*, 405.
- (15) Darensbourg, D. J.; Frost, B. J. Unpublished results.

carbonyl derivatives of nucleobases have previously been reported by Beck and Kottmair.¹⁶ Herein, we wish to describe related chemistry involving thiouracil anionic derivatives of zerovalent tungsten carbonyls. In these instances the thiouracil ligands are bound to the metal center through the exocyclic sulfur initially, with subsequent processes leading to additional binding via one of the ring nitrogen atoms.

Monoanions of uracil derivatives have been shown to exhibit a vast coordination chemistry, binding metals via N(1), N(3), and the exocyclic oxygens (or sulfurs)^{1,2} and, finally, though less common, through C(5).¹⁷ This study will examine the coordination modes and substitution kinetics of two thiouracil derivatives of tungsten(0) carbonyls, specifically 2-thiouracil and 6-methyl-2-thiouracil. HF and DFT theoretical method-



ologies have also been employed in the evaluation of the coordination modes and CO ligand reactivity. Included herein is, to our knowledge, the first crystallographically characterized monodentate sulfur-bound 2-thiouracil anionic metal complex, [Et₄N][W(CO)₅(2-thiouracilate)]. This complex is one of a very few crystallographically characterized transition metal complexes with metal-sulfur interaction having a uracil like backbone, as found via a search of the Cambridge structural database. Of the compounds found in this database search these exist in both the monodentate sulfur bound and the bidentate S, N bound.¹⁸

Experimental Section.

Methods and Materials. All manipulations were performed on a double-manifold Schlenk vacuum line under an atmosphere of argon or in an argon-filled glovebox. Solvents were freshly distilled under nitrogen from sodium-benzophenone ketyl (tetrahydrofuran, hexane, diethyl ether), magnesium iodide (methanol), or phosphorus pentoxide followed by calcium hydride (acetonitrile). Photolysis experiments were performed using a mercury arc 450 W UV immersion lamp purchased from Ace Glass Co. Routine infrared spectra were recorded on a Matteson 6022 spectrometer with DTGS and MCT detectors, using a 0.10-mm CaF₂ cell. Kinetic measurements were monitored on either the Matteson 6022 spectrometer or ASI's ReactIR 1000 system equipped with a MCT detector and 30 bounce SiCOMP in situ probe. ¹H and ¹³C NMR spectra were obtained on a Varian Unity+300 spectrometer and referenced to residual solvent peaks with respect to TMS. ¹³CO was purchased from Cambridge Isotopes and used as received. W(CO)₆ was purchased from Fluka and used without further purification. 2-Thiouracil and 6-methyl-2-thiouracil were purchased from Aldrich Chemical and TCI, respectively, and used without purification. Tetraethylammonium hydroxide 25% w/w in methanol was purchased from Sigma and used as received. Triethyl phosphite was

purchased from Strem, dried over sodium, and distilled prior to use. Microanalyses were performed by Canadian Microanalytical Service, Ltd., Delta, BC, Canada.

Synthesis of [NEt₄][W(CO)₅(L)] (L = 2-Thiouracilate, **1; L = 6-Methyl-2-thiouracilate, **2**).** In a typical synthesis 1.43 mmol of 2-thiouracilate (**1**) or 6-methyl-2-thiouracilate (**2**) was deprotonated with 1.44 mmol of tetraethylammonium hydroxide 25% w/w solution in methanol. This solution was stirred for 30 min followed by the addition of 1.43 mmol of W(CO)₅(MeOH) which was generated photochemically by photolysis of 1.43 mmol of W(CO)₆ in 60 mL of methanol for 1 h. The resulting yellow solution was stirred for 1 h and the solvent removed under vacuum to provide a yellow solid. The yellow solid was washed 3 × 20 mL with hexanes to remove any remaining W(CO)₆ and dissolved in 30 mL of THF. The THF solution was filtered through Celite removing any unreacted [Et₄N][2-thiouracilate] (**1**) or [Et₄N][6-Me-2-thiouracilate] (**2**). Removal of the THF via vacuum left a pure bright yellow powder, 0.59 g (77% yield) of **1** or 0.52 g (62% yield) of **2**. Anal. Calcd for [NEt₄][W(CO)₅(C₄H₃N₂OS)] (**1**), C₁₇H₂₃O₆N₃SW: C, 35.13; H, 3.98; N, 7.23. Found: C, 35.36; H, 4.30; N, 7.51. IR (CH₃CN): 2068 (w), 1922 (s), 1866 cm⁻¹ (m). IR (MeOH): 2065 (w), 1925 (s), 1873 cm⁻¹ (m). ¹³C NMR (CD₃OD, 75 MHz): δ 200.2 (¹J_{C-W} = 127.6 Hz (4 cis CO's), 204.0 (1 trans CO)). Crystals suitable for X-ray diffraction were grown by slow diffusion of diethyl ether into a THF solution of **1** at 0 °C over a period of 5 days. Anal. Calcd for [NEt₄][W(CO)₅(C₅H₅N₂OS)] (**2**), C₁₈H₂₅O₆N₃SW: C, 36.32; H, 4.23; N, 7.06. Found: C, 36.33; H, 4.44; N, 7.28. IR (CH₃CN): 2062.7 (w), 1921.0 (s), 1862.2 cm⁻¹ (m). IR (MeOH): 2063.7 (w), 1923.9 (s), 1873.7 cm⁻¹ (m). ¹³C NMR (CD₃OD/CH₃CN, 75 MHz): δ 200.4 (¹J_{C-W} = 127.6 Hz (4 cis CO's), 204.0 (1 trans CO)).

Synthesis of [NEt₄][W(CO)₄(L)] (L = 2-Thiouracilate, **3; L = 6-Methyl-2-thiouracilate, **4**).** The syntheses of **3** and **4** were conducted in a manner similar to that for **1**. In a typical synthesis 1.44 mmol of 2-thiouracil (**3**) or 6-methyl-2-thiouracil (**4**) was deprotonated with 1 equiv of tetraethylammonium hydroxide 25% w/w in methanol. This solution was stirred for 45 min and taken to dryness, followed by the addition of 5 mL methanol to redissolve the white powder. To this solution was added 1.42 mmol of W(CO)₅THF which was generated photochemically by photolysis of 0.501 g of W(CO)₆ in 60 mL of THF for 45 min. The yellow solution was allowed to stir overnight and evacuated to dryness leaving a yellow powder. Tetrahydrofuran, 20 mL, was added to the solid yielding a yellow brown solution and a yellow powder. The yellow/brown solution was found via IR to be a mixture of W(CO)₅L and W(CO)₄L complexes. The yellow THF insoluble powder was washed with hexanes and dried to yield 0.32 g (40% yield) of **3** as a pure yellow powder. In the case of complex **4** the yellow THF insoluble powder was dissolved in acetonitrile and layered with diethyl ether at -10 °C yielding 0.41 g (52% yield) of **4** as pure yellow crystals. Anal. Calcd for [NEt₄][W(CO)₄(C₄H₃N₂OS)] (**3**), C₁₆H₂₀O₅N₃SW: C, 34.73; H, 4.19; N, 7.59. Found: C, 35.16; H, 4.90; N, 8.08. IR (CH₃CN): 2002.0 (w), 1869.9 (vs), 1848.7 (sh), 1810.1 (m). Anal. Calcd for [NEt₄][W(CO)₄(C₅H₅N₂OS)] (**4**), C₁₇H₂₆O₅N₃SW: C, 35.93; H, 4.61; N, 7.39. Found: C, 35.45; H, 4.41; N, 7.39. IR (CH₃CN): 2002.0 (w), 1871.8 (vs), 1849.6 (sh), 1808.2 cm⁻¹ (m). ¹³C NMR (CD₃OD/CH₃CN, 75 MHz): δ 204.66 (2 cis CO's), 213.97 (1 CO trans N), 216.40 (1 CO trans S). Crystals suitable for X-ray diffraction were grown by slow diffusion of diethyl ether into a CH₃CN solution of **4** at 0 °C over a period of 6 days. However, twinning problems have thus far precluded obtaining a solution of the structure.

Alternative Synthesis of **3 and **4**.** **3** and **4** were prepared thermally by placing 0.15 g of **1** or **2** in 20 mL of CH₃CN. This solution was then heated at 60 °C for 6 h. The yellow solution was then filtered through Celite to remove any decomposition products. The solution was dried in vacuo and washed with 3 × 20 mL of hexanes leaving a bright yellow solid. These complexes displayed infrared spectra identical to those observed for **3** and **4** prepared using the previous described method.

Reaction of **1 and **3** with Triethyl Phosphite.** The reactions of **1** and **3** with triethyl phosphite were carried out in acetonitrile. In a typical reaction approximately 0.05 g of **1** or **3** was dissolved in 2 mL of CH₃CN. To this yellow solution an excess of phosphite was added and the reaction monitored via infrared in the ν(CO) region. The tungsten(0)

(16) Beck, W.; Kottmair, N. *Chem. Ber.* **1976**, *109*, 970.

(17) Hunt, G. W.; Griffith, E. A. H.; Amma, E. L. *Inorg. Chem.* **1976**, *15*, 2993-2997.

(18) (a) Ruf, M.; Weis, K.; Vahrenkamp, H. *Inorg. Chem.* **1997**, *36*, 2130-2137. (b) Cookson, P. D.; Tiekink, E. R. T. *J. Chem. Crystallogr.* **1996**, *24*, 805-810. (c) Garcia-Tasende, M. S.; Suárez, M. I.; Sánchez, A.; Casas, J. S.; Sordo, J.; Castellano, E. E.; Mascarenhas, Y. P. *Inorg. Chem.* **1987**, *26*, 3818-3820. (d) Hunt, G. W.; Griffith, E. A. H.; Amma, E. L. *Inorg. Chem.* **1976**, *15*, 2993-2997. (e) Goodgame, D. M. L.; Rollins, R. W.; Shawin, A. M. Z.; Williams, D. J.; Zard, P. W. *Inorg. Chim. Acta* **1986**, *120*, 91-101. (f) Corbin, D. R.; Francesconi, L. C.; Hendrickson, D. M.; Stucky, G. D. *J. Chem. Soc., Chem. Commun.* **1979**, 248-249.

Table 1. Crystallographic Data for Complex **1**

empirical formula	C ₁₇ H ₂₃ N ₃ O ₆ SW
fw	581.29
space group	P2 ₁ /n
V, Å ³	2112.5(7)
Z	4
d _{calc} , g/cm ³	1.828
a, Å	7.420(2)
b, Å	14.927(3)
c, Å	19.399(4)
β, deg	100.51(3)
T, K	293
μ(Mo Kα), mm ⁻¹	5.604
wavelength, Å	0.710 73
R _F , ^a %	4.99
R _{wF} , ^b %	8.13

$${}^a R_F = \sum |F_o - F_c| / \sum F_o. \quad {}^b R_{wF} = \{[\sum w(F_o^2 - F_c^2)^2] / (\sum wF_o^2)\}^{1/2}.$$

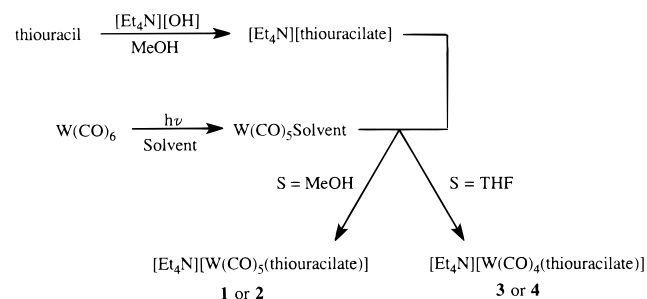
tetracarbonyl complex (**3**) was converted to the product within minutes of addition of the phosphite, whereas complex **1** required a matter of a few hours to be converted to the [NEt₄][*cis*-W(CO)₄(2-thiouracilate)P(OEt)₃] complex. There was virtually no visible change in the solution upon addition of phosphite. Infrared spectra obtained for either reaction were identical: IR (CH₃CN) 2012.0 (w), 1871.8 (vs), 1808.2 (m).

X-ray crystallography. [Et₄N][W(CO)₅(2-thiouracilate)]. Crystal data and details of data collection are given in Table 1. A yellow block of **1** was mounted on a glass fiber with epoxy cement at room temperature. Preliminary examination and data collection were performed on a Siemens P4 X-ray diffractometer (Mo Kα, λ = 0.710 73 Å radiation) for **1**. Cell parameters were calculated from the least-squares fitting of the setting angles for 24 reflections. ω scans for several intense reflections indicated acceptable crystal quality. Data were collected for 3.46 ≤ 2θ ≤ 47.10°. Three control reflections, collected every 97 reflections, showed no significant trends. Background measurements by stationary-crystal and stationary-counter techniques were taken at the beginning and end of each scan for half the total scan time. Lorentz and polarization corrections were applied to 3145 reflections for **1**. A semiempirical absorption correction was applied to **1**. A total of 3143 unique reflections, with |I| ≥ 2.0σ(I), were used in further calculations. The structure of **1** was solved by direct methods [SHELXS programs package, Sheldrick (1993)]. Full-matrix least-squares anisotropic refinement for all non-hydrogen atoms yielded R = 0.0499, R_w = 0.0813, and S = 1.032 for **1**. Hydrogen atoms were placed in idealized positions with isotropic thermal parameters fixed at 0.08. Neutral-atom scattering factors and anomalous scattering correction terms were taken from the *International Tables for X-ray Crystallography*.

Kinetic Measurements. The rate of CO dissociation, chelation, of **1** and **2** was determined by placing 0.10 g of the complex in 15 mL of acetonitrile. These solutions were then placed in a thermostated temperature bath at a variety of temperatures (15, 30, 40, 45, 50, 60 °C for **1** and (15, 27.3, 40, 50, 60 °C) for **2** and stirred via magnetic stirring. Following the E ν(CO) band in **1** and **2** at 1922 and 1921 cm⁻¹, respectively, allowed the conversion of the pentacarbonyl to the product to be monitored.

Kinetic measurements for the conversion of the tetracarbonyl complex (**3**) back to the pentacarbonyl complex (**1**), CO addition, were obtained in analogous manner to that described above. Approximately 0.10 g of **3** was placed in 2 mL of acetonitrile. This solution was then added to the 15 mL of CO-saturated CH₃CN, in a temperature bath. CO was bubbled through the solutions throughout the entire data collection. The rate of CO addition to complex **3** was determined at a variety of temperatures (10, 20, 30, 40 °C). The rates of CO addition kinetics were monitored by following the product appearance in the IR using the intense E ν(CO) band of complex **1** at 1922 cm⁻¹. The CO addition kinetics were also performed at 30 °C as a function of the partial pressure of CO, where P_{CO} = 1.0, 0.75, and 0.50 atm.

The ¹³CO exchange rate for complex **1** was determined by placing an acetonitrile solution of the complex (0.1 g in 20 mL) in a thermostated water bath with magnetic stirring at 30.0 °C. Once thermal equilibrium was reached the solution was placed under an atmosphere

Scheme 1

of ¹³CO. The exchange process was monitored by observing the decrease in absorbance of the highest frequency ν(CO) band of the starting complex **1** as a function of time.

Theoretical Calculations. Theoretical calculations were performed using the Gaussian 94 program package employing the LANL2DZ basis set of Wadt and Hay^{19a} as implemented in Gaussian 94.^{19b} Hartree–Fock (HF) and density functional (DFT) calculations were carried out on all the 2-thiouracilate complexes. DFT calculations were performed using Becke's three-parameter hybrid method²⁰ coupled to the correlation functional of Lee, Yang, and Parr (B3LYP).²¹ Full geometry optimization of **1** was performed starting from the crystal structure of **1**. Complex **3** was optimized starting from a modification of the crystal structure of **1**. Calculations were also performed on potential intermediates by reoptimizing structures of **1** in which one CO had been removed. Frequency calculations were also performed on all 2-thiouracilate complexes including intermediates in order to establish the nature of the extrema and to calculate values for ΔH and ΔG values.

Results and Discussion

The 2-thiouracil derivatives of tungsten hexacarbonyl, complexes **1** and **2**, were synthesized in good yields via displacement of the labile ligand methanol from W(CO)₅(MeOH) (prepared in situ by photolysis of W(CO)₆ in methanol²²) by the tetraethylammonium salt of the corresponding 2-thiouracil (Scheme 1). The protic solvent methanol was employed because of its ability to hydrogen bond to the lone pair of the anionic sulfur donor ligand, thereby negating its CO-labilizing ability.¹¹ On the other hand, the chelated derivatives, **3** and **4**, were synthesized in moderate yields by performing the series of reactions in THF at ambient temperature. Alternatively, complex **1** has been prepared in low yield by deprotonation of the neutral S-bound W(CO)₅(2-thiouracil) derivative with hydroxide.^{16a}

Complexes **1** and **2** exhibit the expected 3-band pattern in the ν(CO) region of the infrared spectra, consistent with the pseudo-C_{4v} symmetry of monosubstituted metal hexacarbonyls. Upon loss of carbon monoxide from these anionic derivatives and subsequent chelation by N(1) (vide infra) of the thiouracil ring (complexes **3** and **4**), a 4-band pattern in the ν(CO) region is observed corresponding to the pseudo-C_{2v} symmetry of a *cis* disubstituted tetracarbonyl complex (Figure 1). It is also evident in Figure 1 that the exocyclic carbonyl substituent shifts to

- (19) (a) Hay, J. P.; Wadt, W. R. *J. Chem. Phys.* **1985**, *82*, 284. (b) Frisch, M. J.; Trucks, G. W.; Schlegel, H. B.; Gill, P. M. W.; Johnson, B. G.; Robb, M. A.; Cheeseman, J. R.; Keith, T.; Petersson, G. A.; Montgomery, J. A.; Raghavachari, K.; Al-Laham, M. A.; Zakrzewski, V. G.; Ortiz, J. V.; Foresman, J. B.; Cioslowski, J.; Stefanov, B. B.; Nanayakkara, A.; Challacombe, M.; Peng, C. Y.; Ayala, P. Y.; Chen, W.; Wong, M. W.; Andres, J. L.; Replogle, E. S.; Gomperts, R.; Martin, R. L.; Fox, D. J.; Binkley, J. S.; Defrees, D. J.; Baker, J.; Stewart, J. P.; Head-Gordon, M.; Gonzalez, C.; Pople, J. A. *Gaussian 94, Revision D.4*; Gaussian, Inc.: Pittsburgh, PA, 1995.
- (20) (a) Becky, A. D. *Phys. Rev. A* **1988**, *38*, 3098. (b) Becky, A. D. *J. Chem. Phys.* **1993**, *98*, 5648.
- (21) Lee, C.; Yang, W.; Parr, R. G. *Phys. Rev. B* **1988**, *37*, 785.
- (22) Darendbourg, D. J.; Meckfessel Jones, M. L.; Reibenspies, J. H. *Inorg. Chem.* **1996**, *35*, 4406.

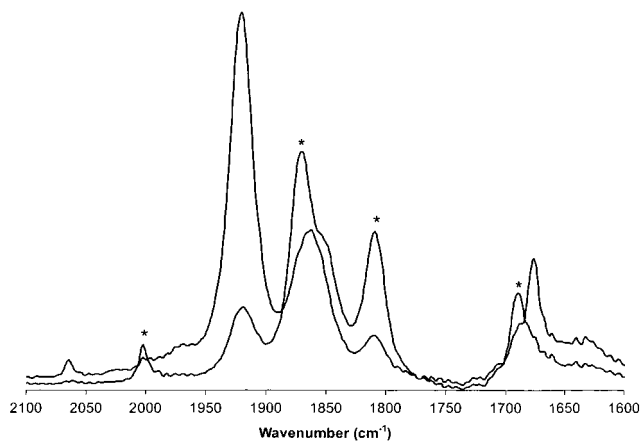


Figure 1. Infrared spectra in $\nu(\text{CO})$ stretching region in acetonitrile for $[\text{Et}_4\text{N}][\text{W}(\text{CO})_5(2\text{-thiouracilate})]$, **1**; and $[\text{Et}_4\text{N}][\text{W}(\text{CO})_4(2\text{-thiouracilate})]$, **3**, in CH_3CN . Peaks with asterisks correspond to those for **3**. The exocyclic carbonyl bands are at 1677 cm^{-1} for **1** and 1690 cm^{-1} for **3**.

higher frequency upon chelation of the thiouracilate ligand. Since the CO stretching vibrations are such good probes of the electronic character of the substituted ligand in metal carbonyl derivatives, it is of interest to compare these parameters observed herein with similar derivatives. Table 2 contains the carbonyl vibrational frequencies for complexes **1–4**, along with those of closely related uracilate, orotate, glycinate, and thiolate tungsten(0) carbonyl derivatives.^{7–10} From these data it is possible to conclude that the ring N(1) donor of the uracilate in the $\text{W}(\text{CO})_5(\text{uracilate})^-$ derivative is more donating than the exocyclic sulfur donor group of the thiouracilate ligands in complexes **1** and **2**.⁷ A similar conclusion can be made with respect to the SPh^- ligand in $\text{W}(\text{CO})_5\text{SPh}^-$, where the $\nu(\text{CO})$ vibrational modes are lower than those in **1** and **2**.⁸ Comparison of the $\nu(\text{CO})$ parameters of complexes **3** and **4** with those of the tungsten tetracarbonyl derivatives of glycinate and orotate leads to similar conclusions.^{7,9–10}

Table 3 summarizes ^{13}C NMR data of the carbonyl ligands in ^{13}C -enriched complexes **1–4**, as well as the corresponding data obtained in our laboratories on similar derivatives. The pentacarbonyl complexes **1** and **2** exhibit the expected two peak pattern in approximately 4:1 intensity ratio, with the more intense ^{13}C resonance due to the four cis carbonyls being observed upfield from the CO group trans to the sulfur donor groups. Coupling constants to ^{183}W , $^1J_{\text{C-W}}$, of 128 Hz were observed for the more intense ^{13}C resonance in both **1** and **2**. The ^{13}C NMR spectra of complexes **3** and **4** each are comprised of three signals in an approximate intensity ratio of 2:1:1, corresponding to one resonance for the two cis CO's and one for each of the other two CO's, trans to nitrogen and trans to sulfur. Both of these latter resonances are slightly downfield from the more intense resonance for the two cis CO ligands. As anticipated from the $\nu(\text{CO})$ parameters, the ^{13}C chemical shifts of the CO ligands for the more electron-donating O- or O,N-ligated complexes are further downfield than the corresponding parameters for the S- or S,N-ligated derivatives.

The solid-state structure of complex **1** was determined by X-ray crystallography. Crystals suitable for X-ray analysis were obtained by the slow diffusion of diethyl ether into a THF solution of the complex maintained at $0\text{ }^\circ\text{C}$ for several days. Crystallographic data and data collection parameters are compiled in Table 1. A thermal ellipsoid view of the monoanion $\text{W}(\text{CO})_5(2\text{-thiouracilate})^-$ is depicted in Figure 2, along with the atomic numbering scheme. Selected bond distances and bond

angles are listed in Table 4. The unit cell for complex **1** also contains a tetraethylammonium counterion to balance the charge. The nearly perfect octahedral environment about the tungsten consists of a 2-thiouracilate anion bound to a tungsten pentacarbonyl fragment through the exocyclic sulfur atom, with a W–S bond length of $2.533(3)\text{ \AA}$. This bond length is similar to the average W–S distance of $2.561(5)\text{ \AA}$ observed in the $\text{W}(\text{CO})_4(\eta^2\text{-S}_2\text{CCH}_3)^-$ anion.²³ The C–S bond distance of $1.709(11)\text{ \AA}$ is indicative of considerable double bond character, in that C–S single bonds are typically $1.817 \pm 0.005\text{ \AA}$ with C=S double bonds being $1.718 \pm 0.005\text{ \AA}$.²⁴

The slight octahedral distortion which exists about the tungsten center results from the positioning of the N(2) atom. That is, the N(2) atom lies between the C(3) and C(4) atoms of the cis carbonyl ligands, which in turn causes an opening of the C(4)–W–C(3) angle to 93.1° with a concomitant closing of the C(3)–W–C(5) and C(4)–W–C(2) angles to 89.7 and 86.3° , respectively. Nevertheless, the N(2) nitrogen is not significantly interacting with either the metal center, C(3), or C(4), with distances of 3.623 , 3.108 , and 3.137 \AA , respectively, which are well beyond the sum of the covalent van der Waals radii of the nuclei. The thiouracilate ligand exhibits a nearly planar pyrimidine ring with a standard deviation from planarity of the ring atoms (plus exocyclic oxygen atom) of 0.0130 \AA , indicative of sp^2 hybridization about the nitrogen atoms. The metal center and the sulfur atom are slightly out of the plane of the pyrimidine ring by 0.0328 and 0.0693 \AA , respectively. The intraligand distances in the 2-thiouracilate are comparable to those observed upon its binding to a variety of other metal centers.² The carbonyl trans to the S exhibits a trans effect; i.e., the W–C bond for the trans CO is shorter than the W–C bond length for the cis CO's ($1.968(11)\text{ \AA}$ for trans and an average distance of $2.058(12)\text{ \AA}$ for cis CO's).

Upon examination of the packing diagram of **1**, it is observed that there is extensive hydrogen bonding between the base pairs, as would be expected for a RNA base pair. Figure 3 depicts a ball-and-stick representation of the hydrogen-bonding motif that exists in the complex. From this figure it is clear that the hydrogen bonding takes place via the N(3) nitrogen and an exocyclic oxygen from a neighboring molecule. This would then indicate that the thiouracilate complex is deprotonated at the N(1) position. The two hydrogen bonds are linear with a distance of 2.882 \AA between the N and O atoms. This distance is in excellent agreement with those previously reported for hydrogen bonding between these base pairs.²⁵ The average deviation from the plane, as defined by the ring atoms of the two uracilate fragments, of the two hydrogen-bound thiouracilate fragments is only 0.0147 \AA , with tungsten and sulfur atoms out of the plane by 0.0274 and 0.0838 \AA , respectively.

Both complexes **1** and **3** underwent ligand substitution reactions with $\text{P}(\text{OEt})_3$ to afford *cis*- $\text{W}(\text{CO})_4(\text{thiouracilate})\text{-P}(\text{OEt})_3^-$ derivatives, albeit at much different rates (Scheme 2). That is, complex **1** reacts with excess $\text{P}(\text{OEt})_3$ in CH_3CN over several hours at ambient temperature, whereas complex **3** affords the same product in minutes under identical reaction conditions. Hence, ring-opening in **3** occurs at the endocyclic nitrogen donor site and this process is more facile than CO loss from complex **1**. When the sequence of reactions in Scheme 2 is carried out with ^{13}C instead of $\text{P}(\text{OEt})_3$, the initially afforded

(23) Darensbourg, D. J.; Wiegrefe, H. P.; Reibenspies, J. H. *Organometallics* **1991**, *10*, 6.

(24) Darensbourg, D. J.; Wiegrefe, H. P.; Wiegrefe, P. W. *J. Am. Chem. Soc.* **1990**, *112*, 9252.

(25) Darensbourg, D. J.; Joyce, J. A.; Bischoff, C. J.; Reibenspies, J. H. *Inorg. Chem.* **1991**, *30*, 1137.

Table 2. Stretching Frequencies of the Carbonyl Ligands in the $W(CO)_5(\text{thiouracilate})^-$ (**1**, **2**) and $W(CO)_4(\text{thiouracilate})^-$ (**3**, **4**) Anions and Related Complexes

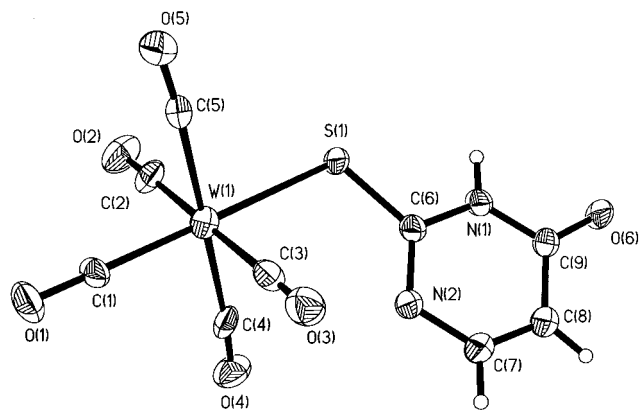
complex ^{a,b}	$\nu(C\equiv O)$, cm^{-1}			ref
$W(CO)_5(2\text{-thiouracilate})^-$ (1)	2063.7 (w) (2064.7)	1922.0 (vs) (1924.8)	1865.0 (m) (1873.7)	<i>c</i> <i>d</i>
$W(CO)_5(6\text{-methyl-2-thiouracilate})^-$ (2)	2062.7 (w)	1921.0 (vs)	1862.2 (m)	<i>c</i>
$W(CO)_4(2\text{-thiouracilate})^-$ (3)	2002.0 (w)	1868.9 (vs)	1848.7 (sh) 1810.1 (m)	<i>c</i>
$W(CO)_4(6\text{-methyl-2-thiouracilate})^-$ (4)	2002.0 (w)	1871.8 (vs)	1849.6 (sh) 1808.2 (m)	<i>c</i>
$W(CO)_5(\text{uracilate})^-$	2065.0 (w)	1917.0 (vs)	1858.0 (m)	3
$W(CO)_5(\text{SPh})^-$	2058.0 (w)	1916.0 (vs)	1855.0 (m)	4
$W(CO)_4(\text{glycinate})^-$	1996.0 (w)	1859.0 (vs)	1849.0 (sh) 1795 (m)	5, 6
$W(CO)_4(\text{orotate})^{2-}$	1987.0 (w)	1842.0 (vs)	1829.0 (sh) 1792 (m)	3

^a As the tetraethylammonium salt. ^b Spectra determined in CH_3CN . ^c This work. ^d Values in parentheses determined in methanol.

Table 3. ^{13}C NMR Data for the Carbonyl Ligands in $W(CO)_5(\text{thiouracilate})^-$ (**1**, **2**) and $W(CO)_4(\text{thiouracilate})^-$ (**3**, **4**) Anions, and Related Complexes

complex	^{13}C resonance, ppm		
	CO- (axial)	CO- (trans to S)	CO- (trans to N)
$W(CO)_5(2\text{-thiouracilate})^-$ (1)	200.2 ^c	204.0	<i>a, b</i>
$W(CO)_5(6\text{-methyl-2-thiouracilate})^-$ (2)	200.4 ^c	204.0	<i>a, b</i>
$W(CO)_4(2\text{-thiouracilate})^-$ (3)	200.2	215.8	213.7 ^{a,d,i}
$W(CO)_4(6\text{-methyl-2-thiouracilate})^-$ (4)	204.7	216.4	214.0 ^{a,d,i}
$W(CO)_5(\text{uracilate})^-$	200.6		205.7 ^{b,e,3}
$W(CO)_5(\text{SPh})^-$	200.7	202.9	<i>a, f, 4</i>
$W(CO)_4(\text{glycinate})^-$	205.5	216.0 ^h	216.8 ^{a,g,i,5,6}
$W(CO)_4(\text{orotate})^-$	205.5	218.0 ^h	218.1 ^{a,g,i,3}

^a As the tetraethylammonium salt. ^b Spectra determined in methanol-*d*₄. ^c ^{13}C - ^{183}W was observed at 128 Hz in the ^{13}C NMR spectrum. ^d Spectra determined in methanol-*d*₄/ CH_3CN . ^e As the PPN salt. ^f Spectra determined in $\text{THF}/(\text{CD}_3)_2\text{CO}$. ^g Spectra determined in CD_3CN . ^h *Trans* to oxygen. ⁱ The assignments of the ^{13}C signals for CO groups *trans* to N vs those *trans* to S or O are based on the general observation that the ^{13}C resonance for the better donor group is in general upfield relative to a weaker donor group in $W(CO)_5$ derivatives (see e.g.: Todd, L. J.; Wilkinson, J. R. *J. Organomet. Chem.* **1974**, *77*, 1. Daresbourg, D. J.; Wiegrefe, H. P. *Inorg. Chem.* **1990**, *29*, 592).

**Figure 2.** Thermal ellipsoid drawing of the anion of complex **1**, along with atomic numbering scheme.

product is the stereoselectively ^{13}C -labeled anion, *cis*- $W(CO)_4(^{13}\text{CO})(\text{thiouracilate})^-$, as evidenced by ^{13}C NMR spectroscopy.

Quantitative kinetic measurements were performed on the CO dissociation processes (**1** \rightarrow **3** and **2** \rightarrow **4**), as well as the reverse process of CO addition (**3** \rightarrow **1**). The rate of CO loss from complexes **1** and **2** with subsequent ring closure via the endocyclic nitrogen was monitored following the disappearance of the intense $\nu(\text{CO})$ modes of the starting complexes in acetonitrile solution using an in situ ReactIR probe. The free carbon monoxide was allowed to escape the reaction solution, thereby allowing the equilibrium depicted in Scheme 3 to proceed to completion. Figure 4 displays the linear plot of \ln

Table 4. Selected Bond Lengths (\AA) and Angles (deg) for **1**^a

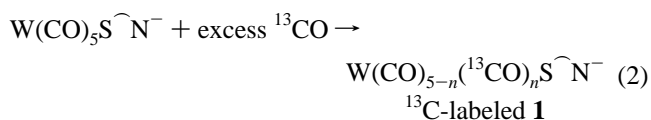
W(1)–C(1)	1.973(11)	O(6)–C(9)	1.252(14)
W(1)–C(5)	2.032(12)	C(7)–C(8)	1.36(2)
W(1)–C(3)	2.066(13)	C(8)–C(9)	1.43(2)
W(1)–C(4)	2.071(12)	N(3)–C(12)	1.491(14)
W(1)–C(2)	2.062(14)	N(3)–C(10)	1.51(2)
W(1)–S(1)	2.553(3)	N(3)–C(16)	1.52(2)
S(1)–C(6)	1.709(11)	N(3)–C(14)	1.541(14)
N(1)–C(9)	1.35(2)	C(12)–C(13)	1.50(2)
N(1)–C(6)	1.374(14)	C(16)–C(17)	1.50(2)
N(2)–C(6)	1.347(14)	C(14)–C(15)	1.49(2)
N(2)–C(7)	1.38(2)	C(10)–C(11)	1.50(2)
C(1)–W(1)–S(1)	179.3(3)	O(6)–C(9)–N(1)	122.3(10)
C(5)–W(1)–S(1)	89.7(3)	O(6)–C(9)–C(8)	124.5(11)
C(3)–W(1)–S(1)	90.3(3)	N(1)–C(9)–C(8)	113.1(10)
C(4)–W(1)–S(1)	90.0(3)	C(12)–N(3)–C(10)	111.8(10)
C(2)–W(1)–S(1)	88.7(4)	C(12)–N(3)–C(16)	109.0(9)
C(6)–S(1)–W(1)	111.9(4)	C(10)–N(3)–C(16)	107.8(9)
C(9)–N(1)–C(6)	126.6(10)	C(12)–N(3)–C(14)	109.2(9)
C(6)–N(2)–C(7)	114.6(9)	C(10)–N(3)–C(14)	108.4(9)
N(2)–C(6)–N(1)	120.4(10)	C(16)–N(3)–C(14)	110.6(9)
N(2)–C(6)–S(1)	123.3(8)	N(3)–C(12)–C(13)	116.3(10)
N(1)–C(6)–S(1)	116.3(8)	C(17)–C(16)–N(3)	115.5(10)
C(8)–C(7)–N(2)	126.3(11)	C(15)–C(14)–N(3)	115.2(10)
C(7)–C(8)–C(9)	118.7(11)	N(3)C(10)–C(11)	116.9(11)

^a Estimated standard deviations are given in parentheses.

[**1**] vs time observed for the reaction involving CO loss in **1** with subsequent chelation of the thiouracilate ring to afford **3**. The temperature-dependent first-order rate constants for **1** \rightarrow **3** and **2** \rightarrow **4** are listed in Table 5. As is readily seen from these kinetic data CO loss occurs about twice as fast in **1** as compared to **3**. That is, CO dissociation is slightly retarded by the presence of the 6-methyl substituent in the thiouracil ring. Eyring plots derived from these data are shown in Figure 5. The activation parameters for CO dissociation were found to be $\Delta H^\ddagger = 83.6 \pm 3.0$ kJ/mol and $\Delta S^\ddagger = -44.9 \pm 9.6$ J/(mol K) for **1** and $\Delta H^\ddagger = 82.0 \pm 3.6$ kJ/mol and $\Delta S^\ddagger = -56.7 \pm 11.6$ J/(mol K) for **2**.

From Scheme 3 the derived rate expression for the disappearance of complex **1** (or **2**) with time is represented by eq 1.

$$-\frac{d[\mathbf{1}]}{dt} = \left\{ \frac{k_1 k_2 + k_{-1} k_{-2} [\text{CO}]}{k_2 + k_{-1} [\text{CO}]} \right\} \{ [\mathbf{1}]_t - [\mathbf{1}]_{\text{equil}} \} \quad (1)$$



Recall that the reactions **1** or **2** \rightarrow **3** or **4**, respectively, were monitored during the early stages of the process under conditions where CO was allowed to escape the reaction solution. Therefore, the rate constant expression in eq 1 reduces to simply k_1 , the rate constant for CO dissociation from complexes **1** and

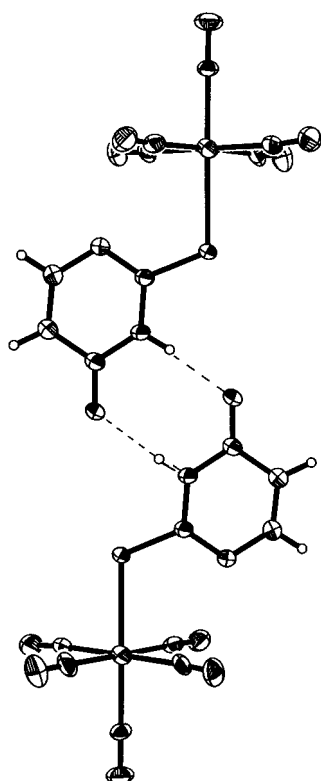
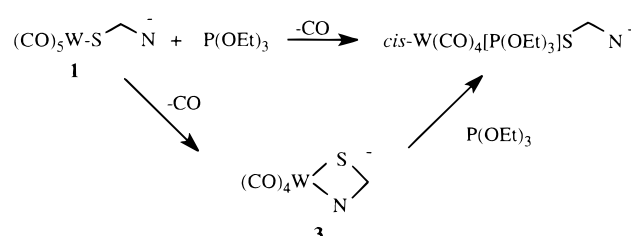
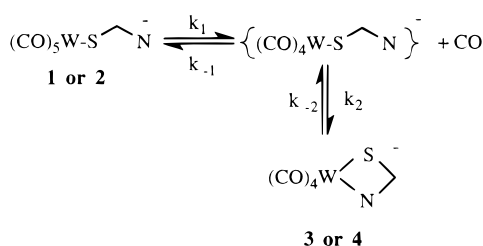


Figure 3. Ball-and-stick representation of **1** showing the hydrogen-bonding network between base pairs.

Scheme 2



Scheme 3



2. We have examined the validity of this assumption by measuring the rate of carbonyl incorporation into complex **1** (eq 2) in the presence of a large excess of the poor nucleophile, ^{13}CO . The first-order rate constant for CO exchange in complex **1** was found to be $1.44 \times 10^{-4} \text{ s}^{-1}$ @ $30.0 \text{ }^\circ\text{C}$, which is slightly larger than the value observed ($1.08 \times 10^{-4} \text{ s}^{-1}$) for $\mathbf{1} \rightarrow \mathbf{3}$. Hence, the suppression of reaction $\mathbf{1} \rightarrow \mathbf{3}$ by the pressure of small quantities of CO in solution is not of major consequences.

The reverse process, i.e., ring-opening of **3** with concomitant addition of CO to afford **1**, has a rate law described by eq 3. This reaction was examined in a CO-saturated acetonitrile solution ($[\text{CO}] < 6.0 \times 10^{-3} \text{ M}$)²⁴ by observing the increase in the most intense $\nu(\text{CO})$ mode at 1921.9 cm^{-1} of the pentacarbonyl product (Figure 6). The temperature-dependent rate constants for $\mathbf{3} \rightarrow \mathbf{1}$ are compiled in Table 6. Under these

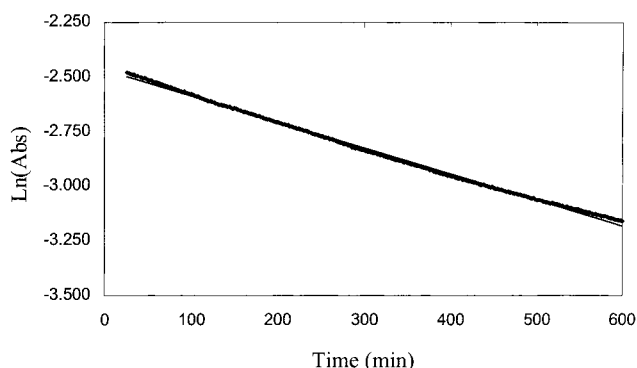


Figure 4. $\ln [\mathbf{1}]$ vs time for the reaction of $\mathbf{1} \rightarrow \mathbf{3}$ at $15 \text{ }^\circ\text{C}$ in acetonitrile.

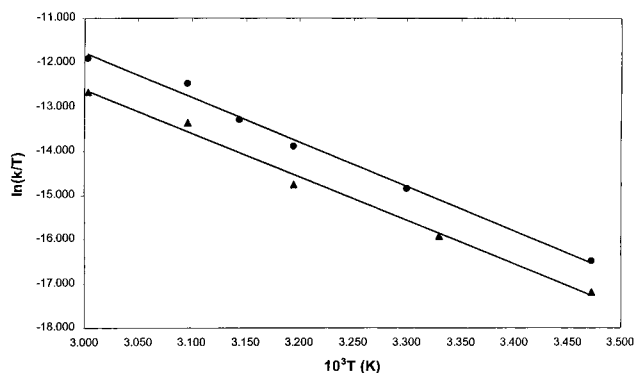


Figure 5. Eyring plots for the conversion of complexes $\mathbf{1} \rightarrow \mathbf{3}$ (●) and $\mathbf{2} \rightarrow \mathbf{4}$ (▲), respectively.

Table 5. Observed First-Order Rate Constants for the Chelation of Complexes **1** and **2** Forming **3** and **4**, Respectively, as a Function of Temperature^a

complex	temp, °C	$10^4 k, \text{ s}^{-1}$	
1	15.0	0.200	
	30.0	1.08	
	40.0	2.90	
	45.0	5.38	
	50.0	12.4	
	60.0	22.8	
2	15.0	0.100	
	27.3	0.367	
	40.0	1.23	
	50.0	5.17	
	60.0	10.6	

^a In CH_3CN .

conditions the reaction arrives at an equilibrium position which favors the $\text{W(CO)}_5(\text{thiouracilate})^-$ anion. An estimate of the equilibrium constant for the process $\mathbf{3} \rightleftharpoons \mathbf{1}$ at ambient temperature is greater than 500 M^{-1} .

$$-\frac{d[\mathbf{3}]}{dt} = \left\{ \frac{k_1 k_2 + k_{-1} k_{-2} [\text{CO}]}{k_2 + k_{-1} [\text{CO}]} \right\} \{ [\mathbf{3}]_t - [\mathbf{3}]_{\text{equil}} \} \quad (3)$$

From the form of the rate constant expression in eq 3 it is possible to deduce that the reverse process, $\mathbf{3} \rightarrow \mathbf{1}$, should be linear in $[\text{CO}]$ at modest CO pressures. Indeed, upon investigation of the reaction as a function of the P_{CO} (1.0–0.5 atm), the observed constant decreased linearly with decreasing partial pressure of carbon monoxide (see Table 6). The composite activation parameters determined for a reaction carried out at 1 atm of carbon monoxide (see Eyring plot in Figure 7) were $\Delta H^\ddagger = 33.1 \pm 1.4 \text{ kJ/mol}$ and $\Delta S^\ddagger = -194.6 \pm 4.7 \text{ J/(mol K)}$.

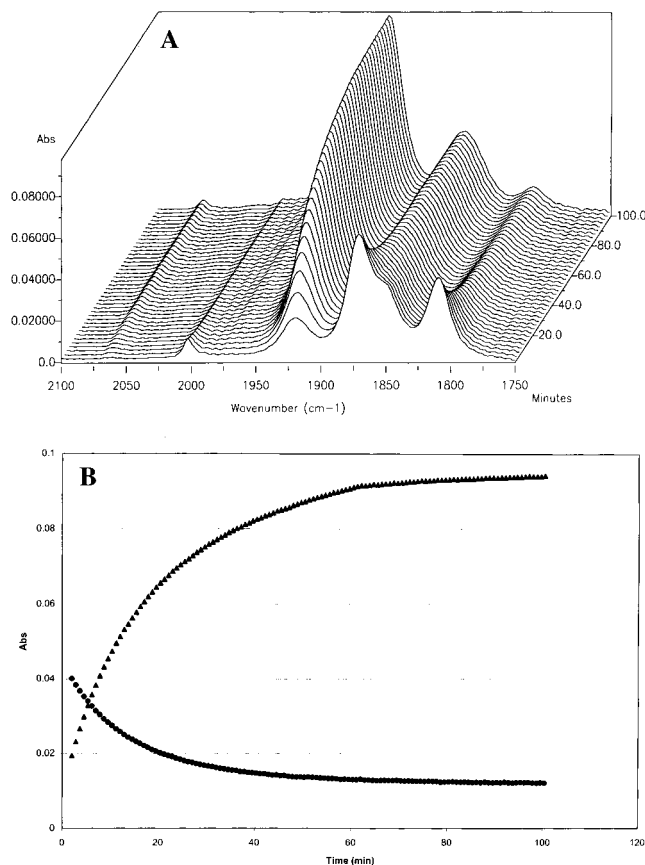


Figure 6. In situ infrared spectral data for the ring-opening process **3** \rightarrow **1** at 30 °C in acetonitrile: (A) spectral changes recorded in the $\nu(\text{CO})$ region during the reaction **3** \rightarrow **1**. (B) Plots of absorbance vs time, where \blacktriangle represents the increase in absorbance of the 1921.9 cm^{-1} band in **1** and \bullet represents the decrease in absorbance of the 1810.1 cm^{-1} band in **3**.

Table 6. Observed First-Order Rate Constants for CO Addition to $[\text{NEt}_3][\text{W}(\text{CO})_4(2\text{-thiouracilate})]^-$ (**3**) as a Function of Temperature under 1 atm of CO^a

temp, °C	$10^4 k_{\text{obs}}, \text{s}^{-1}$	temp, °C	$10^4 k_{\text{obs}}, \text{s}^{-1}$
10.0	3.42	30.0	9.00 ^b
20.0	5.27	40.0	14.3

^a In CH_3CN . ^b $k_{\text{obs}} (\text{s}^{-1}) = 8.07$ and 7.02 for $P_{\text{CO}} = 0.75$ and 0.50 atm, respectively.

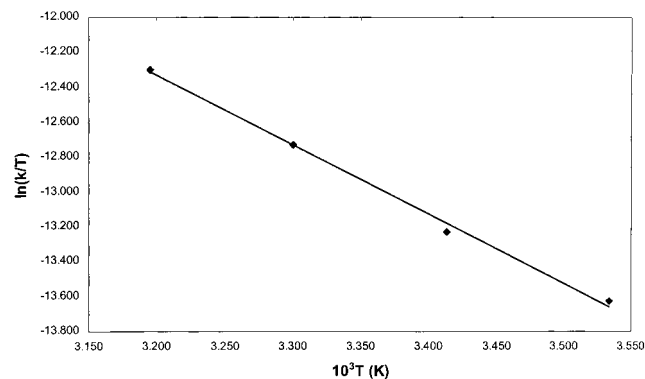


Figure 7. Eyring plot for the conversion of complex **3** \rightarrow **1**.

Theoretical Calculations

Theoretical methodologies were employed in the study of this system for several reasons. That is, calculations were expected to provide valuable information with regard to the stabilities of

Table 7. Comparison of Selected Experimental and Calculated Bond Lengths (\AA) and Angles (deg) in **1**

bond dist/angle	HF	B3LYP	exptl
W–S	2.703	2.681	2.554(3)
W \cdots N	3.676	3.676	3.623
W–C _{trans} –S	1.974	1.969	1.968(11)
W–C _{cis} –N	2.078	2.044	2.073(12), 2.061(13)
W–C _{cis} –S	2.051	2.029	2.059(13), 2.039(11)
S–C	1.778	1.787	1.709(11)
N–W–S	47.8	48.5	48.0
W–S–C	108.6	108.5	111.9(4)
C _{cis} –N–W–C _{cis} –N	89.0	89.4	93.1(4)
C–W–C	90.3	90.2	91.0(5), 89.7(4), 86.3(4)
S–W–C _{trans}	178.0	177.5	179.0(3)
C _{cis} –S–W–S	87.5	87.5	89.9(3), 88.7(4)
C _{cis} –N–W–S	90.0	90.8	90.3(3), 89.8(3)

the possible coordination modes in $\text{W}(\text{CO})_4(2\text{-thiouracilate})^-$ derivatives, as well as the relative thermodynamic parameters of the anions **1** and **3**. In addition, knowledge of the energetics of possible intermediates in the conversion of **1** \rightarrow **3** was anticipated to provide insight into the mechanism of the process. Calculation of intermediates in the reaction is especially important as these are not experimentally observable in most cases and can provide insight into the mechanism of the reaction. Ab initio geometry optimizations were carried out on the system $\text{W}(\text{CO})_5(\text{thiouracilate})^- \rightarrow \text{W}(\text{CO})_4(\text{thiouracilate})^- + \text{CO}$ at the Hartree–Fock (HF) level and at the density functional level using the B3LYP approximation. All computations were performed using effective core potentials with the LANL2DZ basis set available within Gaussian 94. The geometry optimization on all complexes yielded parameters which are consistent with known structures. Table 7 and Figure 8 list calculated structural parameters for complex **1**, along with the experimentally determined values shown for comparison. Both HF and DFT methods gave accurate bond distances and angles for the anion of complex **1**. Figure 8 depicts optimized geometries of the structures relevant to the formation of the product complex **3** via the loss of CO from **1** and subsequent coordination of the endocyclic N(1) group. Figure 9 provides the relative energies of the structures pertinent to the transformation **1** \rightarrow **3** in kJ mol^{-1} . Frequency calculations were also performed on the anionic metal carbonyls, and data obtained in the $\nu(\text{CO})$ stretching region are reported in Table 8 for species **1**, **3**, and **3-INT**. These calculated $\nu(\text{CO})$ values are in good agreement with experimental parameters. Geometry optimizations were also performed on the complexes involved in the conversion of **2** \rightarrow **4**. The energy difference between **2** and **4** was found to be 50.6 kJ mol^{-1} at the HF level. This value is slightly higher than the ΔE between **1** and **3** of 38.3 kJ mol^{-1} . This is consistent with the experimental observation that the rate of conversion of **1** \rightarrow **3** is a factor of 2 times faster than the conversion of **2** \rightarrow **4**.

It is evident from Figure 8 that coordination of N(1) to the tungsten center upon CO loss is computed to be more stable by approximately 53.6 kJ mol^{-1} than coordination via the alternative endocyclic N(3) grouping. This is most likely the consequence of steric hindrance due to the exocyclic oxygen of the uracil ring leading to a longer W–N bond distance (2.285 vs 2.307 \AA). In cases where X-ray structural data are available this is indeed experimentally found to be the case; e.g., 6-methyl-2-thiouracilate is coordinated to Tp^*Zn by way of the exocyclic S and N(1) groups.^{18a} The intermediate which results from dissociation of a CO ligand from the anion of **1**, **3-INT**, exhibits a closer N(1) contact with the cis CO ligand relative to that in the parent species. Hence, it is likely that this represents another case where a chelating ligand assists in the loss of a CO group

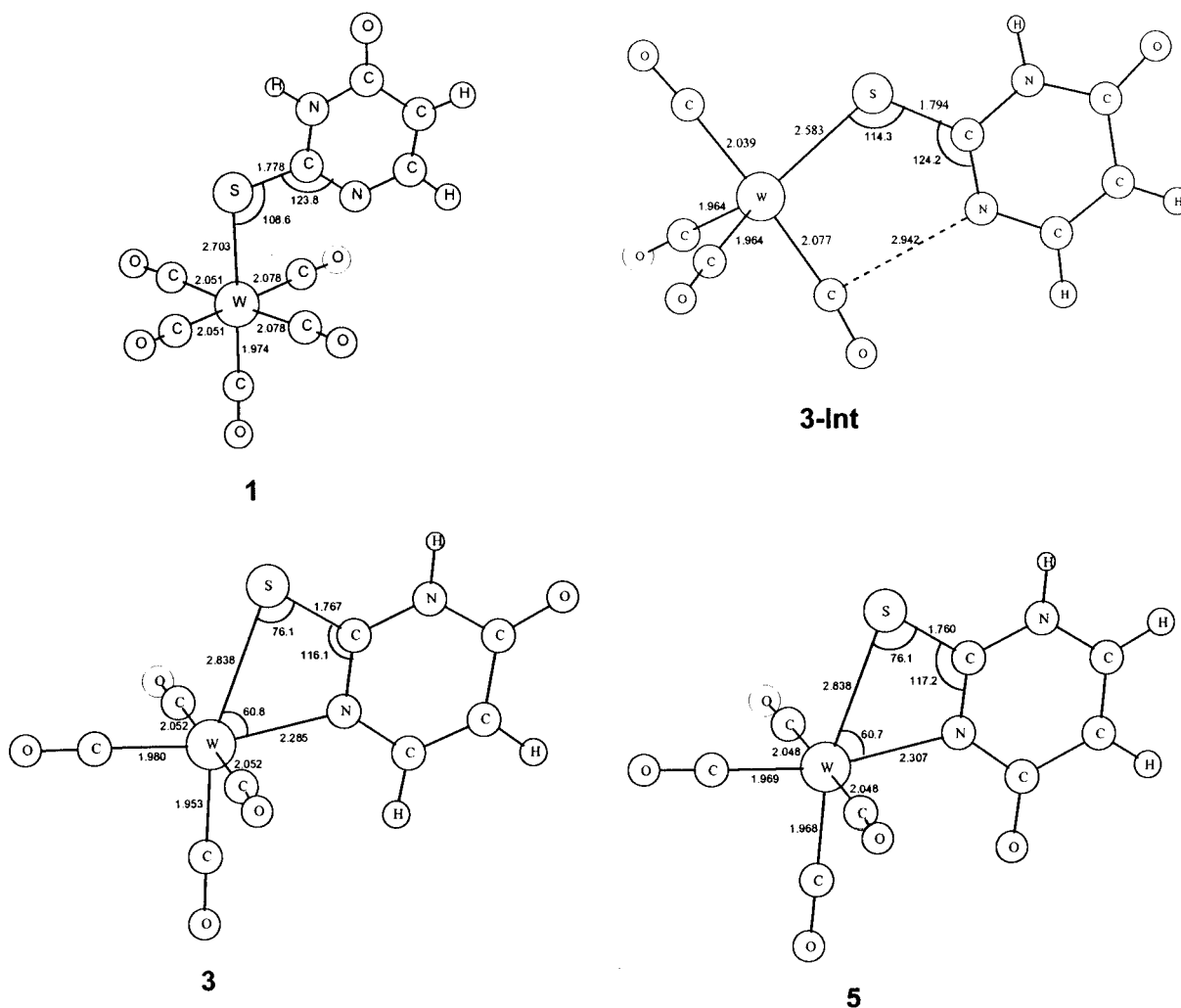


Figure 8. Optimized geometries of the structures relevant to the formation of complex **3** from **1**. In addition the structure for the alternative nitrogen chelate is depicted in **5**. Bond lengths are in Å, and angles, in deg.

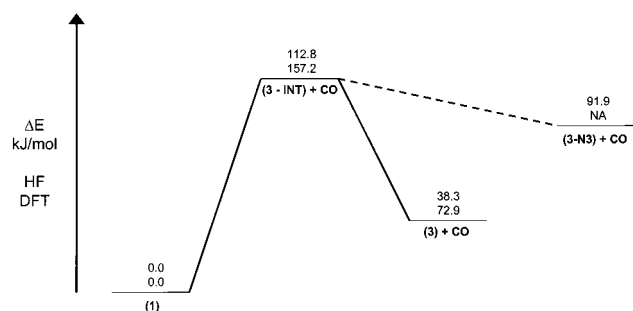
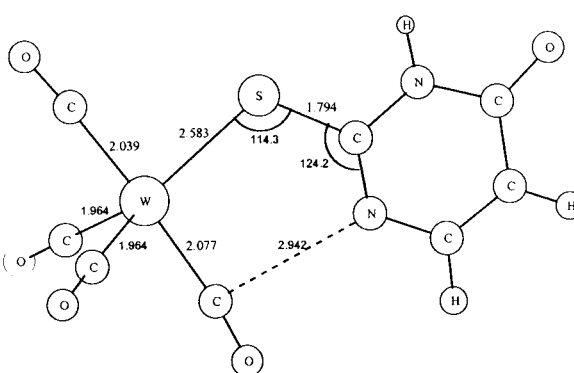
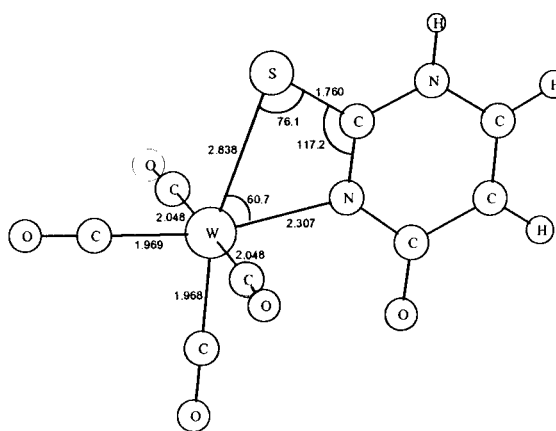


Figure 9. Energy profiles for the two alternative pathways for complex **1** undergoing ring-closure with endocyclic nitrogen binding. The energies are in kJ mol^{-1} .

in octahedral metal carbonyls. For example, a similar kinetic effect is noted in $\text{W}(\text{CO})_5\text{O}_2\text{CR}^-$ anions, where interaction of the distal oxygen atom of the carboxylate with the cis CO ligands lead to enhanced CO dissociation.^{24,25} At the same time there is significant shortening of the W–S bond upon CO dissociation, going from 2.703 Å in **1** to 2.583 Å in **3-INT**. This would be anticipated based on the S group serving as a π -donor in the 16-electron intermediate resulting from CO dissociation.²⁶ It is also worth noting that the calculated ΔG value (1.03 kJ/mol at the HF level and 37.7 kJ/mol at



3-Int



5

the DFT level) is slightly positive in proceeding from **1** to **3** + CO, consistent with experimental observations of 5.90 kJ/mol.

The energy of the intermediate, **3-INT**, is calculated to be significantly higher in energy (135 kJ/mol vs 82 kJ/mol) than the activation energy determined experimentally for the transformation of **1** \rightarrow **3**. This suggests that the transition state and concomitantly **3-INT** are stabilized via interactions with the solvent molecule, acetonitrile. Indeed, we have previously measured the activation enthalpy for dissociation of CH_3CN in the neutral *fac*- $\text{W}(\text{CO})_3(\text{CH}_3\text{CN})(\text{dppm})$ derivative to be 98 ± 6 kJ/mol.²⁷ Therefore, the expected binding of the CH_3CN ligand to the anionic complex described herein is expected to be less than 98 kJ/mol. To examine this proposal we have measured the rate of conversion of **1** \rightarrow **3** in the much weaker coordinating solvent, nitrobenzene. A first-order rate constant of $1.67 \times 10^{-6} \text{ s}^{-1}$ at 30 °C was measured which is 2 orders of magnitude slower than the corresponding value in CH_3CN of $1.08 \times 10^{-4} \text{ s}^{-1}$. This observation clearly illustrates the important role of solvent in assisting the CO loss process. Computations are currently underway in our laboratories to investigate the transition states and intermediates for the conversion of **1** \rightarrow **3** in the presence of coordinating solvents in an effort to better understand the potential energy surface of this reaction.

(26) Sellmann, D.; Wille, M.; Knoch, F. *Inorg. Chem.* **1993**, 32, 2534.

(27) Darensbourg, D. J.; Zalewski, D. J.; Plepyd, C.; Campana, C. *Inorg. Chem.* **1987**, 26, 3727.

Table 8. Calculated $\nu(\text{CO})$ Stretching Frequencies for Complexes **1**, **3**, and **3-INT**

	1		3		3-INT
	calc (rel int)	exp (rel int)	calc (rel int)	exp (rel int)	calc (rel int)
$\nu(\text{C}\equiv\text{O}), \text{cm}^{-1}$	2002 (91)	2064 (w)	1950 (237)	2002 (w)	1961 (195)
	1912 (209)		1832 (720)	1869 (vs)	1852 (2031)
	1874 (2240) }	1922 (vs)	1831 (2577)	1849 (sh)	1833 (914)
	1871 (2134) }		1797 (1315)	1810 (m)	1810 (1443)
	1837 (1175)				

^a Calculations were performed at the DFT using the LANL2DZ basis set and B3LYP functionals and are unscaled.

Conclusion

The synthesis and X-ray structure of the exocyclic sulfur ligated 2-thiouracilate derivatives of tungsten pentacarbonyl are described herein. In the solid state, two $\text{W}(\text{CO})_5(2\text{-thiouracilate})^-$ anions are associated by way of two hydrogen bonds between the metal-bound nucleobases ($\text{N}\cdots\text{O} = 2.882 \text{ \AA}$). On the other hand, in dilute methanol solution the individual anions are hydrogen-bonded to the alcohol as evidenced by a shift to higher frequencies of the $\nu(\text{CO})$ modes. The 2-thiouracilate and 6-methyl-2-thiouracilate pentacarbonyl complexes were shown to readily undergo stereoselectivity *cis* CO dissociation with concomitant formation of the exocyclic sulfur/endocyclic N(1) chelated tetracarbonyl derivatives. Under an atmosphere of carbon monoxide the tungsten pentacarbonyl anion is slightly more stable than its tetracarbonyl counterpart. The kinetic

parameters for CO dissociation from the $\text{W}(\text{CO})_5(2\text{-thiouracilate})^-$ anions support a mechanism where the incipient 16-electron species is stabilized by π -donation from the thiolate ligand. Ab initio calculations carried out for the pentacarbonyl \rightleftharpoons tetracarbonyl + CO processes at the Hartree-Fock and DFT levels, support these experimental observations.

Acknowledgment. Financial support of this research by the National Science Foundation (Grants 96-15866 and 95-28196) and the Robert A. Welch Foundation is greatly appreciated.

Supporting Information Available: X-ray crystallographic files in CIF format for the structure determination of **1**. This material is available free of charge via the Internet at <http://pubs.acs.org>.

IC990758N